Diffusion-controlled crystal growth in deeply undercooled $Zr_{50}Cu_{50}$ melt on approaching the glass transition

Q. Wang,[1] Li-Min Wang,[1] M. Z. Ma,[1] S. Binder,[2] T. Volkmann,[2] D. M. Herlach,[2]
J. S. Wang,[3] Q. G. Xue,[3] Y. J. Tian,[1] and R. P. Liu[1,*]

[1]*State Key Lab of Metastable Materials Science and Technology, Yanshan University, Qinhuangdao, Hebei 066004, China*
[2]*Institut für Materialphysik im Weltraum, Deutsches Zentrum für Luft- und Raumfahrt, D-51170 Köln, Germany*
[3]*Department of Metallurgy, University of Science and Technology Beijing, Beijing 10081, China*

(Received 17 November 2010; published 12 January 2011)

Crystal-growth velocity in metallic melts has been reported by others to increase monotonically with undercooling. Nevertheless, such an observation is not predicted by conventional growth theory. In this work, the metallic melt of $Zr_{50}Cu_{50}$ is studied to address the problem by measuring the growth velocity over a wide range of undercooling up to 325 K. A maximum growth velocity is observed at an undercooling of 200 K instead of the monotonic increase reported in the literature. We find that the planar or dendrite growth theories can explain the value of the maximum growth velocity, but the predicted location of the maximum in undercooling is far less than that seen by experiment. With the assistance of current results, a general pattern of crystal growth is established for melts of a variety of substances, where all sluggish crystal-growth kinetics is explained by the diffusion-controlled mechanism at deep undercooling.

DOI: 10.1103/PhysRevB.83.014202 PACS number(s): 64.70.pe, 61.43.Dq, 66.20.−d, 81.10.Aj

I. INTRODUCTION

Detailed knowledge of crystal growth from undercooled melts is required for the development of a comprehensive understanding of the formation of metastable crystalline structures, although crystal growth has no bearing on the glass-forming ability of metallic melts.[1] The underlying physical processes in crystal growth include the nature of the crystal-liquid interface, the thermodynamic driving force, and the transport mechanisms of mass and heat in the liquid.[2] Models have been developed to describe crystal growth in undercooled melts of metals[3] with isotropic bondings, as well as for covalent and molecular systems with strong anisotropic bondings.[4] For the Zr-based alloys with glass-forming ability that are of present interest, there is isotropic bonding due to *s* electrons and additionally anisotropic bonding contributed by *d* electrons.

Growth kinetics in undercooled melts of metals and alloys is largely measured in the range where the kinetics is driven by a strong temperature gradient in front of the solid-liquid interface. A continuous increase of growth rate with undercooling ΔT is invariably observed experimentally in metallic melts, even in Si and Ge. This occurs despite the fact that large undercoolings of about 20% of the melting temperature are achieved by containerless processing techniques.[1] From a more fundamental point of view, there should be a temperature in the range between the liquidus, T_L, and the glass-transition temperature, T_g, at which the effect of the growing driving force for crystallization and the effect of a progressively increasing viscosity on growth kinetics should compensate each other, leading to a maximum in the growth velocity V at some temperature between T_L and T_g. The unusual continuous increase of growth velocity observed in undercooled metallic melts needs to be explained. The glass-transition temperatures of pure metals and solid solutions are expected from empirical rules to be about one-third of the liquidus temperature.[5] Therefore, the undercooling at which the maximum in $V(\Delta T)$ should appear is far away from the undercooling range accessible by undercooling experiments, even if levitation techniques are utilized. Notwithstanding, this is not the case for glass-forming metallic melts.[6]

In the present work, we report measurements of crystal-growth velocity on $Zr_{50}Cu_{50}$ alloy melts undercooled by electromagnetic levitation. This alloy shows glass-forming ability with a high glass-transition temperature of $T_g/T_m \approx 0.56$ ($T_g \approx 673$ K and $T_m = 1208$ K).[7] Moreover, the $Zr_{50}Cu_{50}$ alloy is an equiatomic compound with chemical stoichiometry, which melts congruently. The alloy is compatible with the requirements of the electrostatic levitation technique, and large undercoolings are achieved. We present measurements of the growth velocity of an alloy melt undercooled containerlessly by electrostatic levitation over a large undercooling range. We present experimental evidence for the existence of a maximum in the growth-velocity–undercooling relation. The compilation of crystal-growth kinetics for various types of melts supports a general pattern.

II. EXPERIMENTAL DETAILS

$Zr_{50}Cu_{50}$ samples were prepared by argon-arc melting and alloying the components of Zr and Cu with a purity of 99.999%. Prior to the melting of the two metals, titanium was burned essentially to reduce the residual oxygen in the chamber. An electrostatic levitation facility was used to undercool bulk samples containerlessly with diameters of 2–3 mm under ultrahigh-vacuum conditions.[8] Temperature was measured without contact by a two-color pyrometer with an absolute accuracy of ±5 K. The advancement of the solidification front during solidification was directly observed by a high-speed camera (Photron Fastcam Ultima APX) with a maximum frame rate of 3000 pictures per second. The growth velocity V is determined by the relation $V = s/\Delta t$, where s is the solidification path and Δt is the time interval during which picture frames are taken. The measurement technique and the geometrical analysis of the solidification

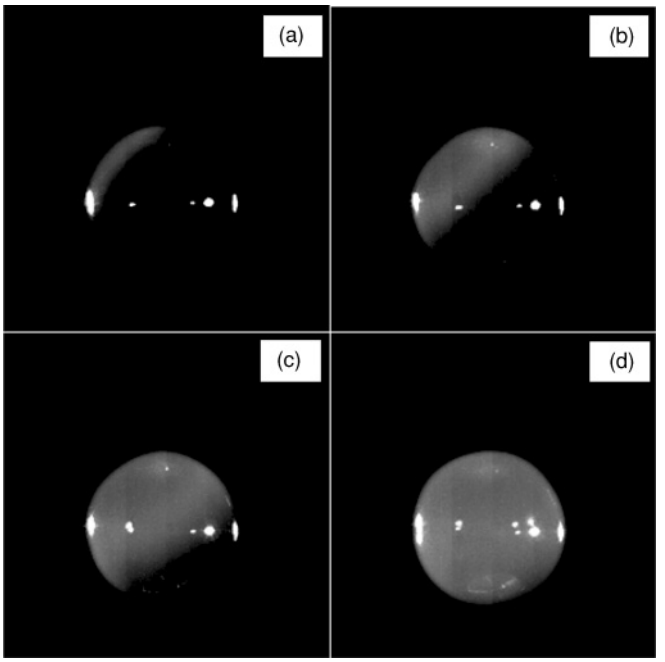

FIG. 1. Solidification processes of the $Zr_{50}Cu_{50}$ alloy triggered at a undercooling of 180 K. The images were taken by a high-speed camera at a rate of 3000 frames/s. The light areas are due to the latent heat released from the crystallization. The advancement of the solid-liquid interface is visible from parts (a)–(d).

front advancing through the undercooled melt have been given in detail elsewhere.[9] The viscosity of the $Zr_{50}Cu_{50}$ melt at high-temperature regions was determined with a rotating cylinder method by using an RTW-04 physical property analyzer of melts. The heat of fusion of $Zr_{50}Cu_{50}$ was determined in a Netsch STA449 C differential scanning calorimeter with a cooling and subsequent heating cycle at a rate of 2.5 K/min in the temperature range of 1088–1328 K, i.e., 120 K below and above the melting point of $T_m = 1208$ K.

III. RESULTS AND DISCUSSION

The solidification process of the undercooled $Zr_{50}Cu_{50}$ melt is illustrated in Fig. 1 at a undercooling ΔT of 180 K by taking photographs of levitated drops at various time intervals during solidification with a high-speed camera. The latent heat generated upon solidification raises the temperature of the solidified phase, which can be seen as the bright areas, while the dark areas represent the undercooled liquid phase. The solid-liquid interface becomes obvious, and the interface front propagates continuously with time, as shown in Figs.1(a)–1(d). Figure 2 shows the dependence of the growth velocity V on undercooling ΔT up to 325 K. The maximum undercooling corresponds to a temperature of the undercooled melt of 883 K, about 210 K higher than the glass temperature $T_g \approx 673$ K. A maximum in the growth-velocity–undercooling relation is observed at an undercooling of $\Delta T \sim 200$ K (or $0.83T_m$). The highest growth rate, 0.025 m/s, is two to three orders of magnitude lower than those of Ni or Si melts,[10,11] albeit much higher than those of some glass-forming oxides and organic liquids.[12,13]

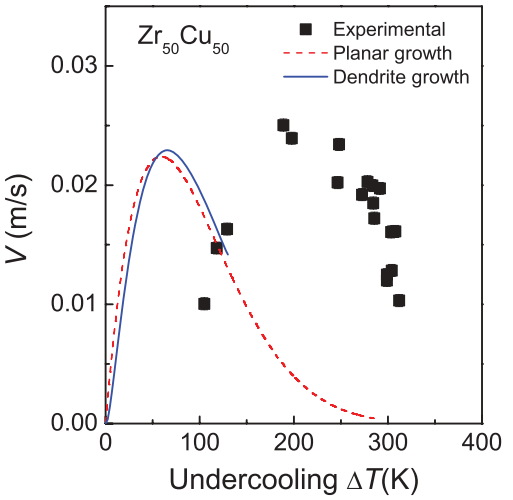

FIG. 2. (Color online) Undercooling ΔT dependence of crystal-growth rate V of the $Zr_{50}Cu_{50}$ alloy. The lines are based on the planar and dendrite growth theories.

Since $Zr_{50}Cu_{50}$ is a congruently melting stoichiometric compound, crystals grow by the formation and propagation of dendrites. Sharp interface theory of dendrite growth is usually applied to analyze the experimental results, as the total undercooling ΔT is expressed as the sum of several contributions,[3] $\Delta T = \Delta T_k + \Delta T_t + \Delta T_r + \Delta T_c$. Here, $\Delta T_k = T_m - T_i$ (T_i denotes the interface temperature) is the kinetic undercooling of the solid-liquid interface, and ΔT_t, ΔT_r, and ΔT_c are the thermal, curvature, and solutal undercoolings, respectively. The curvature undercooling is given by the expression $\Delta T_r = 2\Gamma/R$, where Γ is the Gibbs-Thomson coefficient and R is the curvature radius at the tip of a dendrite. Since $Zr_{50}Cu_{50}$ melts congruently, the solutal undercooling vanishes, $\Delta T_c \approx 0$. The curvature undercooling, ΔT_r, is usually small compared with thermal undercooling and kinetic undercooling, that is, $\Delta T_r \ll \Delta T_t$ and $\Delta T_r \ll \Delta T_k$, especially if thermal dendrites are considered to be congruently melting as in the present work. The thermal undercooling is computed by the solution of the thermal transport equation, yielding $\Delta T_t = \Delta T_{\text{hyp}} Iv(Pe_t)$. On the right-hand side of the preceding equation, the first term is given by $\Delta T_{\text{hyp}} = \Delta H_m / C_p^l$, where ΔH_m is the heat of fusion and C_p^l is the specific heat of the undercooled liquid. The second term Iv is the Ivantsov function. The third term Pe_t is the thermal Peclet number given by the expression. $Pe_t = (VR)/2D_T$, where D_T is the thermal diffusivity. The total undercooling is consequently approximated by $\Delta T \approx \Delta T_t + \Delta T_k$ in the range $\Delta T \leqslant \Delta T_{\text{hyp}}$ and $\Delta T \approx \Delta T_k$ in the range $\Delta T \geqslant \Delta T_{\text{hyp}}$.[3] At large undercoolings, in particular if the temperature of the melt is decreasing further toward the glass temperature, the diffusion coefficient and the viscosity become strongly temperature-dependent and, consequently, in the conventional practice of writing V as the product, $V \approx \mu \Delta T_k$, μ will not be a constant, but will be temperature-dependent.

According to recent studies of crystal-growth dynamics at a planar solid-liquid interface, the growth velocity V is determined by the relation[4]

$$V = A\eta^{-\xi}[1 - \exp(-\Delta G/RT)], \quad (1)$$

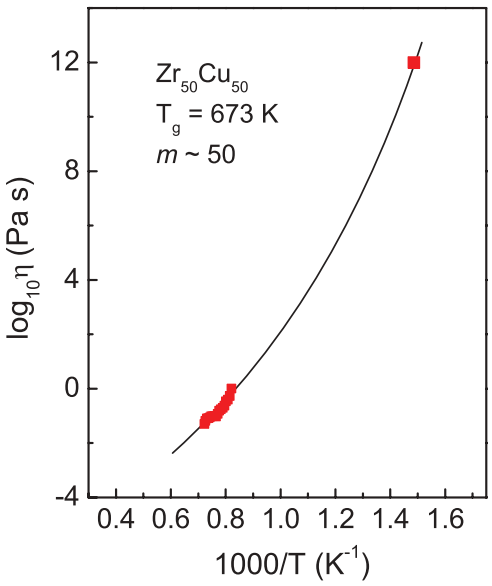

FIG. 3. (Color online) Viscosity of $Zr_{50}Cu_{50}$ melt. The low-temperature viscosity is assigned on the basis of the empirical expression of 1012 Pa s at T_g. The line is plotted from the fit to the data in terms of the VFT equation $\log_{10}\eta = -6.6 + 5361/(T - 383)$.

where A is $d\eta_0^{\xi}\tau_0^{-1}\exp(-\Delta S_m/R)$, η is the viscosity, d is the molecular diameter, $\eta_0 = 10^4$ Pa s, τ_0 is the structural relaxation time at $\eta = \eta_0$, ΔS_m is the entropy of fusion, ΔG is the Gibbs free-energy difference between crystal and liquid, and ξ is a material-specific constant. τ_0 can be assessed from the Maxwell relation, $\tau = \eta/G_\infty$, where G_∞ is the high-frequency shear modulus of liquid. The heat of fusion ΔH_m of $Zr_{50}Cu_{50}$ is determined to be 119 J/g (or 9.2 kJ/mol), giving $\Delta S_m = 7.6$ J/mol K. Figure 3 illustrates the measured viscosity of the $Zr_{50}Cu_{50}$ melt as a function of temperature. The viscosity at T_g [673 K Ref. 7] is assigned with the empirical relation that upon glass transition the viscosity reaches 10^{12} Pa s.[14] The Vogel-Fulcher-Tammann equation, $\eta = A\exp[B/(T - T_0)]$, is used to model the viscosity data with A, B, and T_0 being constants, and the fit gives $\log\eta = -6.6 + 5361/(T - 383)$. ξ is reported to depend on the fragility of the liquid by the relation $\xi = 1.1 - 0.005m$, where m is the fragility index.[4] Liquid fragility quantifies the change of viscosity or structural relaxation time with T_g-scaled temperature at $T = T_g$, and is defined by $m = [d\log\eta/d(T_g/T)]_{T=T_g}$.[14] The fragility index of the $Zr_{50}Cu_{50}$ melt is calculated to have the value of $m = 50$, comparable to those of Vit 1 and Vit 4.[15] This value is slightly lower than the reported value of 62.[7,16] For the dendrite growth mode, Eq. (1) has to be rewritten using the linear approximation, $\Delta G = \Delta S_m \Delta T$,[17] and the replacement of ΔT by ΔT_k, generating the expression $V = [(A\eta^{-\xi}\Delta S_m)/RT]\Delta T_k$. The calculated curves in terms of planar and dendrite growth modes are presented in Fig. 2. The numerical values used for the calculations are summarized in Table I from our work and previous results of Refs. 18–23.

The two growth modes quantitatively reproduce the maximum growth velocity of ~0.025 m/s in the undercooled $Zr_{50}Cu_{50}$ melt. However, a large extra undercooling of 127 K remains. The thermal contribution in the dendrite growth mode

TABLE I. Parameters used in the calculation of dendrite growth velocity in $Zr_{50}Cu_{50}$ melt. ΔH_m is the heat of fusion, C_p^l is the liquid heat capacity, T_m is the melting point, D_T is the thermal diffusivity, V_m is the mole volume, Γ is the Gibbs-Thomson coefficient, a is the average atomic distance, d is the average atomic diameter, G_∞ is a high-frequency shear modulus, and ξ is a material-specific coefficient.

Parameters	Values	Refs.
ΔH_m (J/mol)	9219	This work
C_p^l (J/mol K)	45[a]	18, 19, and 20
T_m (K)	1208	19
D_T (m^2/s)	3e-6[b]	21 and 22
V_m (m^3/mol)	1.05e-5	23
Γ (K m)	1.4e-7	this work
d (m)	3.3e-10	19 and 23
G_∞ (Pa)	3.13e10	19
ξ	0.85	This work

[a]This is an average on the basis of the reported results of similar composition.
[b]This value is referred from the measurements of Vit 1 Ref. 21 and $Zr_{55}Cu_{30}Al_{10}Ni_5$.[22]

cannot generate the large undercooling, since the extreme low growth velocity generates a low thermal Peclet number Pe_t and a subsequent Ivantsov function Iv. In addition, a low hypercooling limit $\Delta T_{\rm hyp} \approx 205$ K is found for $Zr_{50}Cu_{50}$, and that is a relatively small value of all alloys investigated so far and much smaller than the hypercooling limit of the solid solution of Co-Pd alloys.[24] Likewise, the curvature contribution ΔT_r cannot offer such high undercooling, and an extra contribution needs to be involved within the framework of sharp interface theory of dendrite growth.

A comparison of the growth kinetics in deeply undercooled melts of various materials requires a scaling temperature. Using a melting point to scale temperature, the data of $Zr_{50}Cu_{50}$ melts are thus replotted against $T_{cr} = T/T_m$ in Fig. 4 together with the data of other materials, including Ni,[10] Si,[11] Ge,[25] o-terphenyl,[26] tri-α-naphthylbenzene,[12] Li_2O-$2SiO_2$,[27] and MgO-CaO-$2SiO_2$.[28]. A feature clearly visible in Fig. 4 is that the crystal-growth kinetics in the semiconductor and metallic melts in the intermediate undercooling region assumes a plateaulike dependence. A change from the sharp maximum for the molecular and oxide melts to the plateaulike maximum for semiconductor and metallic ones is exhibited in a general pattern by various melts.

Equation (1) emphasizes that at deep undercoolings, the viscosity-related kinetics dominates the planar growth kinetics.[4] Similarly, the behavior is also predicted by the dendrite growth theory in the sense that if the undercooling of the melt reaches the hypercooling limit $\Delta T_{\rm hyp}$, the absolute stability of a thermal dendrite is reached, resulting in a planar interface at $\Delta T > \Delta T_{\rm hyp}$ with $\Delta T_t = 0$. A complete construction of the growth kinetics in the $Zr_{50}Cu_{50}$ melt in the whole undercooling region requires low-temperature data. The growth rate at T_g can be roughly evaluated by referring to the studies of $Zr_{65}Cu_{35}$ Ref. 29 and $Zr_{50}Co_{50}$,[30] where the growth rates are in an order of magnitude of 10^{-9}m/s near their glass transitions. As the entropy of fusion of $Zr_{50}Cu_{50}$ is considered, a value of $10^{-9.2}$m/s is derived

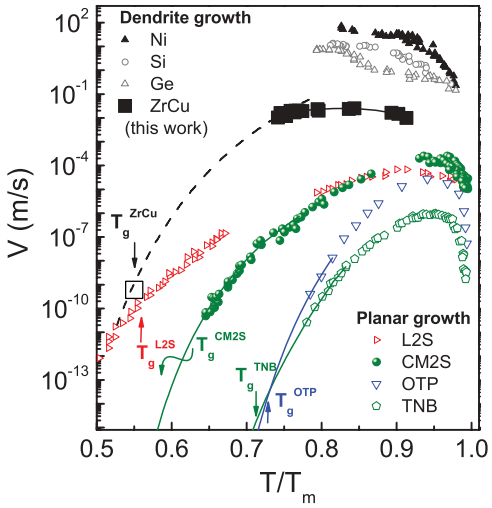

FIG. 4. (Color online) Crystal-growth rates of various liquid materials, elements (Ni, Si, and Ge), alloys ($Zr_{50}Cu_{50}$), small molecular liquids [o-terphenyl (OTP) and tri-α-naphthylbenzene (TNB)], and oxides [Li_2O-$2SiO_2$ (L2S) and CaO-MgO-$2SiO_2$ (CM2S)]. The temperature is reduced by the melting points T_m. The value of $Zr_{50}Cu_{50}$ at glass transition is based on the results of $Zr_{65}Cu_{35}$ and $Zr_{50}Co_{50}$ melts. The crystal-growth rates at low temperature near the glass transition (thin solid lines and thick dashed line) are guided by kinetically controlled processes.

at T_g,[31] as marked in Fig. 4 by an open square. Strikingly, the expression $V \propto \eta^{-\xi}$ which is similar to Eq. (1), restores well the experimental measurements for the $Zr_{50}Cu_{50}$ melt, as shown by the thick dashed line in Fig. 4 Note that compared with Eq. (1), a factor of 70 is required here. This might partly come from the error in the calculation of the growth velocity at T_g. The bottom line from the present work is that the growth velocity of the glass-forming metallic $Zr_{50}Cu_{50}$ melt indeed couples with the viscosity at the low-temperature regime on approaching the glass transition, in analogy to the molecular and oxide melts, where the growth rates exhibit a similar temperature dependence as the viscosity in various substances (cf. the Angell plot[14]). Assuming the validity of the Einstein-Stokes relation, the growth kinetics in the $Zr_{50}Cu_{50}$ melt is diffusion-limited in the deeply undercooled region near T_g. Finally, it is worthwhile to emphasize that the growth rates in the metallic melts start to decouple from viscosity at a lower temperature $\sim 0.73T_m$, in contrast to molecular and oxide systems, in which the two are coupled up to temperatures approaching $0.9T_m$.

IV. CONCLUSIONS

In summary, the crystal-growth velocity in the deeply undercooled $Zr_{50}Cu_{50}$ melt has been measured, and the growth kinetics is constructed across a wide undercooling range from the liquidus to the glass-transition temperature. A maximum crystal-growth velocity is successfully observed. Planar and dendrite growth theories fail to explain the experimental observation. A general pattern of crystal-growth kinetics is presented for various types of undercooled melts, where the diffusion-controlled mechanism still accounts for the crystal-growth kinetics at the deeply undercooled region.

ACKNOWLEDGMENTS

This work was supported by the National Basic Research Program of China (973 Program No. 2010CB731604), the NSFC (50821001/50731005/10804093/51071138), the Program for New Century Excellent Talents in University (NECT-09–0118), and a research grant from DAAD, Germany.

*Corresponding author: riping@ysu.edu.cn

[1] D. M. Herlach, P. Galenko, and D. Holland-Moritz, *Metastable Solids from Undercooled Melts*, edited by R. Cahn, Pergamon Materials Series (Pergamon, Amsterdam, 2007).
[2] K. A. Jackson, Interface Sci. **10**, 159 (2002).
[3] W. Kurz and D. J. Fisher, *Fundamentals of Solidification*, 4th ed. (Trans Tech, Zurich, 1998).
[4] M. D. Ediger, P. Harrowell, and L. Yu, J. Chem. Phys. **128**, 034709 (2008).
[5] D. Turnbull, Contemp. Phys. **10**, 473 (1969).
[6] W. L. Johnson and K. Samwer, Phys. Rev. Lett. **95**, 195501 (2005).
[7] W. H. Wang, J. J. Lewandowski and A. L. Greer, J. Mater. Res. **20**, 2307 (2005).
[8] T. Meister, H. Werner, G. Lohoefer, D. M. Herlach, and H. Unbehauen, Eng. Practice **11**, 117 (2003).
[9] H. Assadi, S. Reutzel, and D. M. Herlach, Acta Mater. **54**, 2793 (2006).
[10] O. Funke, G. Phanikumar, P. K. Galenkoa, L. Chernova, S. Reutzel, M. Kolbe, and D. M. Herlach, J. Cryst. Growth **297**, 211 (2006).
[11] C. Panofen and D. M. Herlach, Mater. Sci. Eng. A **669**, 449 (2007).
[12] J. H. Magill and D. J. Plazek, J. Chem. Phys. **46**, 3757 (1967).
[13] G. W. Scherer and D. R. Uhlmann, J. Cryst. Growth **29**, 12 (1975).
[14] C. A. Angell, K. L. Ngai, G. B. McKenna, P. F. McMillan, and S. W. Martin, J. Appl. Phys. **88**, 3113 (2000).
[15] M. D. Demetriou, J. S. Harmon, M. Tao, G. Duan, K. Samwer, and W. L. Johnson, Phys. Rev. Lett. **97**, 065502 (2006).
[16] S. N. Yannopoulos and G. P. Johari, Nature (London) **442**, E7 (2006).
[17] C. V. Thompson and F. Spaepen, Acta Metall. **27**, 1855 (1979).
[18] A. I. Zaitsev, N. E. Zaitseva, Y. P. Alekseeva, E. M. Kurilćhenko, and S. F. Dunaev, Inorg. Chem. **39**, 816 (2003).
[19] G. J. Fan, M. Freels, H. Choo, P. K. Liaw, J. J. Z. Li, Won-kyu Rhim, W. L. Johnson, P. Yu, and W. H. Wang, Appl. Phys. Lett. **89**, 241917 (2006).
[20] T. Abe, M. Shimono, M. Ode, and H. Onodera, Acta Mater. **54**, 909 (2006).
[21] M. Yamasaki, S. Kagao, Y. Kawamura, and K. Yoshimura, Appl. Phys. Lett. **84**, 4653 (2004).
[22] M. Yamasaki, S. Kagao, and Y. Kawamura, Script. Mater. **53**, 63 (2005).

[23]N. Mattern, A. Schöps, U. Kühn, J. Acker, O. Khvostikova, and J. Eckert, J. Non-Cryst. Solids **354**, 1054 (2008).

[24]T. Volkmann, G. Wilde, R. Willnecker and D.M. Herlach, J. Appl. Phys. **83**, 3028 (1998).

[25]S. E. Battersby, R. F. Cochrane, and A. M. Mullis, Mater. Sci. Eng. A **226**, 443 (1997).

[26]R. J. Greet and J. H. Magill, J. Phys. Chem. **71**, 1746 (1967); D. J. Plazek, C. A. Bero, and I.-C. Chay, J. Non-Cryst. Solids **181**, 172 (1994).

[27]T. Fuss, C. S. Ray, C. E. Lesher, and D. E. Day, J. Non-Cryst. Solids **352**, 434 (2006).

[28]V. M. Fokin, M. L. F. Nascimento, and E. D. Zanotto, J. Non-Cryst. Solids **351**, 789 (2005).

[29]J. Saida, M. Matsushita, C. Li, and A. Inoue, Mater. Sci. Eng. A **304–306**, 338 (2001).

[30]U. Köster and J. Meinhardt, Mater. Sci. Eng. A **178**, 271 (1994).

[31]The data analyses of the molecular and oxides materials in Fig. 4 indicate that the systems with similar structure and kinetic properties such as fragility and T_g/T_m have comparable growth rates at T_g's. This conclusion can also be derived on the basis of the studies in Ref. 4 [Eq. (5)].